CRD-2019-3-42 Revise manuscript (minor revisions)

Assessment of biventricular function by three-dimensional speckle tracking echocardiography in adolescents and young adults with human immunodeficiency virus infection: A pilot study.

Lidia Capotosto, MD, Gabriella D'Ettorre, MD, Camilla Ajassa, MD, Nelson Cavallari, MD, Maria Rosaria Ciardi, MD, Giuseppe Placanica, MD, Serafino Ricci, MD, Pietro Lucchetti, MD, Gaetano Tanzilli, MD, Enrico Mangieri, MD, Carlo Gaudio, MD, Vincenzo Vullo, MD, Antonio Vitarelli, MD, FACC – Sapienza University, Cardiology and Infectious Diseases Depts, Rome, Italy

Running title: HIV-LV-RV-3DSTE

Presented in part at the EuroEcho meeting, Milan, Italy, December 5-8, 2018

Word count: 4598

Address for correspondence:
Antonio Vitarelli, M.D.
Via Lima 35
00198 Rome, Italy
telephone number: 39/6/85301427,
FAX number: 39/6/8841926,
E-mail: vitar@tiscali.it
cardiodiagnostica@gmail.com

Abstract

Background. The purpose of the study was to assess biventricular parameters of wall deformation with three-dimensional speckle tracking echocardiography (3DSTE) in adolescents and young adults with human immunodeficiency virus infection (HIV) on antiretroviral therapy in order to detect a possible subclinical myocardial dysfunction.

Methods. Twenty-one patients aged 12 to 39years with HIV, 21 normal controls of the same age and sex, and 21 patients with idiopathic non-ischemic dilated cardiomyopathy (DCM) were studied with 3DSTE. All HIV patients were stable in terms of HIV infection, with no history of heart disease or other chronic systemic disease except HIV infection, and were on highly active antiretroviral therapy (HAART) with good immunological control. Standard echocardiographic measures of LV-RV function were assessed. 3D LV global longitudinal strain (GLS), circumferential strain, radial strain and LV twist (TW) were calculated. Global area strain (GAS) was calculated by 3DSTE as percentage variation in surface area defined by the longitudinal and circumferential strain vectors. 3D right ventricular (RV) global and free-wall longitudinal strain were obtained.

Results. LV GLS and GAS were lower in HIV patients compared to normal controls ($p=0.002$, and $p=0.01$, respectively). There were no significant differences in LV ejection fractions between the groups. There was a weak positive correlation between LV GLS and age ($r=0.215$, $p=0.034$) and a weak negative correlation between LV GLS and nadir-CD4 T-cells count ($r=0.198$, $p=0.043$). DCM patients had more marked and widespread reduction in LV GLS and GAS compared to controls ($p<0.001$), whereas in HIV patients LV strain impairment ($p<0.05$) was more localized in basal and apical regions. RV free-wall longitudinal strain was significantly reduced in HIV patients when compared with the control group ($p=0.03$). No patient had pulmonary systolic pressure higher than 35mmHg.

Conclusions. Three-dimensional speckle tracking echocardiography may help to identify HIV patients at high cardiovascular risk allowing early detection of biventricular dysfunction in the presence of normal LV ejection fraction and in the absence of pulmonary hypertension. LV strain impairment in HIV patients is less prominent and widespread compared to DCM patients.

Key words: Human immunodeficiency virus infection, echocardiography, three-dimensional speckle tracking echocardiography, left ventricular function, right ventricular function.

People living with human immunodeficiency virus (HIV) have a high risk for cardiac disease, including myocarditis, cardiomyopathy, pericarditis, valvular disease, and pulmonary hypertension (1). With the advent of highly active antiretroviral therapy (HAART), there has been a shift from severe dilated cardiomyopathy to mildly reduced LV systolic function, often minimally symptomatic, or various degrees of impaired diastolic function (2-5). Despite these improvements, evidence from both industrialized and developing countries (3,4) suggests that the prevalence of subclinical LV dysfunction in patients with well-controlled HIV infection may approach 50% and represent a newly recognized comorbid condition.

Adult studies have shown that asymptomatic HIV-infected patients manifest mild functional and morphologic cardiac changes (5-7), in addition to lipid and metabolic derangements, both with and without HAART. Also antiretroviral-naïve and antiretroviral-exposed HIV-infected children have been shown to have cardiac abnormalities on echocardiography (8,9), the most common being left ventricular (LV) dilation and LV hypertrophy.

Two-dimensional speckle tracking echocardiography (2D-STE) has emerged as a new means of assessment of myocardial wall movements and deformation (10,11) and more sensitive compared to ejection fraction in detecting early changes in ventricular performance(12-15). 2D-STE capability is limited by the changes in heart morphology during the cardiac cycle and the difficulty in tracking speckles in different frames because of out of plane motion. The newly developed three-dimensional speckle tracking echocardiography(3D-STE) provides quick and comprehensive quantitative assessment of ventricular myocardial dynamics and was applied in various pathological conditions(16,17) but never in HIV patients during HAART treatment. Accordingly, the goals of this analysis were: 1) to determine early changes in global and segmental left(LV) and right(RV) ventricular function with 3D speckle-tracking echocardiography(3DSTE) in young patients with HIV; 2) to compare these changes with the 3DSTE findings in patients with idiopathic non-ischemic dilated cardiomyopathy and severe systo-diastolic dysfunction; 3) to assess strengths and limitations of 3DSTE compared to 2DSTE.

Methods.

Population. We enrolled 21 patients infected with HIV(mean age 23.9±3.7 years): 5 adolescents(age 12-18 years) and 16 young adults(age 19-39 years). Most of these patients(17/21, 81%) acquired the disease from their mothers antenatally. The study was a retrospective cross-sectional one involving patients recruited from the HIV clinics in both pediatric and adult Infectious Disease Departments. All patients had normal ejection fraction (>55%) and sinus rhythm at the time of the echocardiographic study and were on antiretroviral treatment per protocol of the Infectious Disease Departments. None had a NYHA (New York Heart Association) functional class >2. DAD risk score was assessed taking into account age, gender, total and HDL cholesterol, smoking status (current or past), blood pressure, history of diabetes, family history of CVD, and exposure to indinavir, lopinavir and abacavir (18). Patients with coronary artery disease, moderate or greater valvular heart disease, atrial fibrillation, congenital heart disease, obesity(body mass index $\geq$30kg/m^2), chronic obstructive pulmonary disease, endocrinological, liver, kidney, or neoplastic diseases were excluded from the study. Twenty-one healthy age and sex-matched subjects who were seen at the Echo-lab for routine check-ups or sport activities and had normal physical, electrocardiographic and echocardiographic findings were recruited as controls. To better understand the magnitude and distribution pattern of ventricular strain impairment in HIV-infected patients, we selected as further controls twenty-one patients with previously diagnosed idiopathic non-ischemic dilated cardiomyopathy, aged 20-44 years, who presented with severe LV systo-diastolic dysfunction and strain reduction. All these patients had: 1) LV end-diastolic dimension >112% of the predicted value, corrected for age and body surface area; (2) left ventricular ejection fraction (LVEF) <50%; 3) NYHA classification ≥IIgrade; 4) no significant coronary artery stenosis on coronary angiography. The study was approved by the local Institutional Research Committee. All patients gave written consent.

Echocardiography. Patients were examined in the left lateral decubitus position using a Vivid E9 commercial ultrasound scanner(GE Vingmed Ultrasound AS, Horten, Norway) with

phased-array transducers. Grayscale recordings were optimized at a mean frame rate of ≥50 frames/sec. Measurements of cardiac chambers were made by transthoracic echocardiography according to established criteria(19,20). LV ejection fraction by modified biplane Simpson method and mass index were estimated(19). LV deceleration time (DT) and right ventricular systolic pressure(RVSP) were determined(21). Mitral and tricuspid annular velocities(S_a, E_a, A_a) were measured at the lateral corner of the mitral annulus on the transthoracic four-chamber views using spectral Doppler myocardial imaging. The mitral and tricuspid E to E_a ratio(E/E_a) were used as indices for LA and RA pressure(22).

Two-dimensional speckle tracking echocardiography. LV two-dimensional longitudinal strain (Figure 1) was calculated in three apical views in relation to the strain value at aortic valve closure and measured in 17 segments on the basis of the software bull's-eye diagram. Strain values were not derived in the presence of more than two suboptimal segments in a single apical view. Longitudinal systolic deformation was characterized as shortening, and systolic indices provided negative values. Circumferential and radial systolic strains were calculated as an average of strain values obtained from the basal, mid, and apical parasternal short-axis views. Manual readjustments were made only when necessary to ensure accurate tracking.

To assess regional and global RV systolic function in the longitudinal direction, we adopted a 6-segment RV model (basal RV lateral wall, mid RV lateral wall, apical RV wall, apical septum, mid septum, and basal septum). Peak systolic strain was recorded for the 3 RV myocardial free wall and septal segments and the entire RV wall. The following measurements were obtained: RV GLS= global right ventricular longitudinal strain; RV FWLS= free wall right ventricular longitudinal strain. Global strain was calculated by averaging local strains along the entire right ventricle using machine software (EchoPAC BT13, GE Vingmed Ultrasound, Horten, Norway).

Three-dimensional speckle tracking echocardiography. The original raw data from three-dimensional data sets were examined on a separate software workstation(EchoPAC BT13, 4D Auto-LVQ, GE Vingmed-Ultrasound, Horten, Norway). Ventricular alignment was accomplished in apical

and short axis views. For end-diastolic volumes, a point was placed at the center of the mitral annular plane and a second point at the LV apex to generate an end-diastolic endocardial border tracing including the papillary muscles inside the LV cavity. For the end-systolic volumes, the same process was made in end-systole and acquisition of LVEF and volumes was determined. The correct endocardial alignment during the cardiac cycle was verified and volume waveforms were obtained. A second semiautomated epicardial tracking was made to delineate the region of interest for LV mass and strain analysis. The software provided segmental longitudinal, circumferential, radial, and 3D strain time curves, from which peak global strain and averaged peak strain at three LV levels (basal, midventricular, and apical) were obtained. Global longitudinal strain(GLS), global circumferential strain(GCS), global area strain(GAS), and global radial strain(GRS) were determined. Global area strain was calculated as the percentage change in endocardial surface area from its original dimensions. LV twist (TW) was defined as the net difference(in degrees) of apical and basal rotation at isochronal time points(23). The 3D data sets were displayed as multi-planar reconstruction images in three short-axis slices from apex to base and apical four-chamber and two-chamber views. Adjustments were made in the multi-planar reconstruction images until the landmarks (mitral valve, LV apex, and aortic valve) were well positioned in each standard view. The software automatically generated LV basal and apical rotation angles and LV twist time curves, from which peak basal rotation, peak apical rotation, and peak LV twist were obtained. LV torsion was the normalized twist by the LV length from apex to the base. Peak diastolic untwisting velocity and time to peak untwisting velocity were measured. Peak untwisting velocity(PUV) was determined as the greatest negative deflection following peak twisting velocity. Time to peak untwisting velocity was measured from the QRS onset as the time to reach peak value. Global strain values were not determined in the presence of more than 3(of 17) uninterpretable segments. A final 17-segment bull's-eye map of strain values was displayed(Figure 1).

Three-dimensional RV speckle tracking echocardiography was carried out by imaging the RV chamber in apical views by using a 4V phased array transducer with high volume rate(≥30 image

frames/sec) and six-beat acquisition with a methodology previously described (17,24). The transducer was positioned at the modified apical position (more lateral than that in the standard apical view) for full RV coverage. RV analysis was performed using multiple reference points all over the endocardial contour in order to obtain a 3D ventricular tracing in long-axis and short-axis views. RV three-dimensional global longitudinal strain was determined using the Echo PAC BT13. 3D longitudinal strain of RV free-wall only (FW LS) was then calculated (Figure 1).

Stress-echo test. Symptom-limited or submaximal (up to 85% of the age-predicted maximum heart rate) exercise stress-echo test (25) was performed using a reclining ergometer, with initial workload set at 25 W and 25 W increments every 2 minutes. Heart rate and rhythm were recorded by 12-lead ECG, and blood pressure was measured manually during the last 30 seconds of each stage by sphygmomanometry. Exercise testing was interrupted for chest pain, severe systemic hypertension, significant ventricular arrhythmia, or muscular exhaustion. Regional wall motion was assessed visually (25). Functional and echocardiographic parameters were determined at peak effort. Ischemia was defined as the development of new or worsening wall motion abnormalities with exercise, with the exception of isolated hypokinesia of the basal inferior and basal inferoseptal segments. Resting and exercise strain images were then transferred to the Echopac work station and analyzed off-line.

Statistics. Categorical variables are presented as numbers and percentages and continuous data are expressed as mean ± SD. Linear correlations, univariate and multivariate analysis were used for comparisons. Echocardiographic parameters of LV-RV function(standard, 3DSTE) were compared between groups using Student's unpaired t tests. Differences among three or more groups were assessed using one-way analysis of variance with post hoc comparisons by Bonferroni test. Differences were considered statistically significant when the p value was <0.05. Intra- and inter-observer variability of strain measurements was evaluated in 10 randomly selected patients. To analyze intraobserver variability, measurements of strain parameters were made at multiple sites in different patients on 2 different occasions. For interobserver variability, a second investigator randomly made measurements at the above different sites without knowledge of other

echocardiographic parameters. The intraobserver and interobserver variabilities were determined as the absolute difference between each observer's value divided by the mean of both measurements and expressed as a percentage (coefficient of variation). For the assessment of reproducibility of measurements intra-class correlation coefficients were also calculated with good agreement defined as having a coefficient >0.80.

Results.

Feasibility. Sixty-three subjects were included in the study (21 HIV-positive patients, 21 patients with non-ischemic dilated cardiomyopathy and 21 healthy controls). Ninety four subjects were initially evaluated. Six patients were excluded from the study due to coexistent disease. LV and RV 3DSTE measurements from all segments were not feasible in a total of 25 subjects (8 and 17 subjects respectively) due to inadequate myocardial tracking. The overall feasibility of LV 3DSTE was 89%(63/71), and overall feasibility of RV 3DSTE was 79%(63/80).

Clinical data. Baseline characteristics of HIV patients and controls are summarized in Table 1. No differences were present between the two groups of patients in body mass index, body surface area, heart rate, and blood pressure. We found a trend toward an increase in systemic blood pressure in HIV patients but the difference did not reach statistical significance.

Standard echocardiographic data. Conventional 2D echocardiographic data are presented in Table 2. There was no significant difference in LV ejection fraction and RV fractional shortening between HIV patients and controls. HIV patients had increased mean LVMI, MV E/E_a and TV E/E_a compared to controls.

Comparison of HIV strain data with healthy controls. Three-dimensional speckle tracking echocardiographic parameters are summarized in Table 3. 3D LV GLS, LV GAS and TW were lower in HIV patients compared to normal controls (p=0.002, p=0.01, and p=0.03, respectively). There were no significant differences in LV ejection fractions between the groups. 8/21 (38%) HIV patients had 3D LV GLS <-18% (lower limits of the normal range). There was a weak direct correlation between

LV GLS and mean wall thickness(r=0.365, p<0.01), a weak positive correlation between LV GLS and age (r=0.215, p=0.034), and a weak negative correlation between LV GLS and nadir-CD4 T-cells count (r=0.198, p=0.043). There was no significant relation between 3DSTE parameters and the duration of the disease.

Peak rotation and twist were lower compared to controls. In HIV patients there was a weak direct correlation between LV GLS and apical rotation(r=0.314, p<0.01), and a weak inverse correlation between LV GLS and twist(r=-0.331, p<0.01).

RV free-wall longitudinal strain was significantly reduced in HIV patients when compared with the control group (p=0.03). No patient had pulmonary systolic pressure higher than 35mmHg. 3/21 (14%) HIV patients had 3D RVFWLS >-22% (lower limits of the normal range). No patient with LV GLS >-18% had RVFWLS >-22% or significant difference in any other measure of RV function.

LV GLS and GCS measured by 2DSTE and 3DSTE showed significant correlations between both methods (respectively, r=0.87, p<0.001, and r=0.82, p<0.005). No significant correlation between GRS extracted from 3DSTE and from 2DSTE was obtained. The 3DSTE approach gave lower values than 2DSTE (Table 3) for both GLS and GCS components (mean absolute difference of 1.8% between the two modalities).

The total duration of 3D data analysis averaged 9.2±1.3 min, which was 46% less than the time used for 2D analyses (14.4±2.6min, p<0.005). Both image acquisition time (2.7±0.6min vs 4.4±1.2min, p<0.001) and offline analysis time (6.5±0.6min vs 10.4±2.1min, p<0.005) were significantly faster for 3DSTE compared with 2DSTE. Analysis time included calculation of LV volumes, LVEF, and all three (2D) or four (3D) strains from a single vendor-specific algorithm.

Stress-echo data. All HIV patients had negative stress-echo test for coronary artery disease. Patients with regional strain impairment at rest had no significant rest and exercise wall motion abnormalities or additional exercise strain abnormalities.

Comparison of HIV strain data with DCM values. Table 4 shows the differences in segmental 3D left ventricular strain in controls, HIV-positive patients and patients with idiopathic non-ischemic dilated cardiomyopathy (DCM). DCM patients had more marked and widespread reduction in LV GLS compared to controls ($p<0.001$), whereas in HIV patients LV LS impairment ($p<0.05$) was more localized in basal and apical regions.

The peak systolic strain in various planes had some regularities in normal controls, as radial strain was the largest in the mid region and smallest in the apical region, whereas longitudinal and circumferential strains were the largest in the apical region and smallest in the basal region ($p<0.05$). This regularity was not evident in the DCM group, since there were severe diffuse strain impairment and no significant differences between different planes (p=NS). An intermediate pattern was shown in HIV patients, with moderate strain impairment, mainly in the basal and apical segments.

Reproducibility. The intra-inter-observer variability was slightly higher for 2D GLS, GCS and GRS compared to the corresponding 3D strain values (Table 5). Intra-observer and inter-observer coefficients of variation for LV measures ranged from 3% up to 7%, and from 4% up to 9%, respectively, and for RV measures ranged from 4% up to 9%, and from 5% up to 12%, respectively. Intra-observer and inter-observer intraclass coefficients were for LV measures from 0.84 to 0.96, and from 0.82 to 0.91, respectively, and for RV measures from 0.83 to 0.92, and from 0.78 to 0.87, respectively.

Discussion

The major findings of the present study were: 1) 3DSTE parameters show global biventricular dysfunction in HIV-infected patients in the presence of normal ejection fraction; 2) LV strain impairment is less prominent and widespread compared to patients with idiopathic non-ischemic dilated cardiomyopathy; 3) RV dysfunction is detectable in the absence of pulmonary hypertension; 4) overall, 3DSTE allows to identify early myocardial changes in HIV patients better than 2DSTE.

Cardiac abnormalities in HIV-positive patients could be attributed to a direct HIV effect on the heart, to opportunistic infections afflicting the heart directly or indirectly, or to the effects of HAART either directly on myocardial cells and endothelial function or indirectly through derangement of the lipid profile causing premature atherosclerosis. Risk factors such as smoking, hypertension, dyslipidemia or diabetes mellitus can also be commonly found in HIV patients. Because it is possible that more than one of these factors is present in a given patient, a multifactorial pathogenesis should be considered (4).

Biventricular strain in HIV-infected group. In our cohort of young HIV patients with low prevalence of traditional cardiovascular risk factors, the prevalence of 3D ventricular strain impairment was significantly higher than in uninfected controls. HIV may trigger mechanisms leading to cardiac dysfunction. Several studies suggest that cardiac dysfunction in persons living with human immunodeficiency virus is associated with HAART (1,9,26). Whereas impairment of conventional echocardiographic measures of LV ejection fraction and fractional shortening is usually a late index of cardiac dysfunction, 3D speckle-tracking-derived strain and twist are new sensitive parameters of ventricular function that can give us insight into whether these patients are at higher risk for cardiovascular disease despite having been treated with antiretroviral drugs and despite being asymptomatic.

In vitro and in vivo studies validated 3DSTE against reference techniques such as sonomicrometry and magnetic resonance imaging tagging (27). Age-related studies have been reported (28). Both 2DSTE and 3DSTE showed to be more sensitive to identify subtle myocardial damage compared to standard indices of LV function (29-31). Advantages and disadvantages of 3D over 2D speckle tracking have been previously discussed (16,17). The 3D mode avoids foreshortening of apical views, consumes less time in data acquisition and offline-analysis, helps to solve the 2D problem of out-of-plane motion by tracking motion of speckles in all three dimensions, allows to analyze a greater percentage of segments than 2DSTE, and is superior to 2D analysis in terms of intra-observer and inter-observer variability. However, this advantage is realized at the price of lower

frame/volume rate and temporal resolution, higher dependence on image quality and possible dropouts in the endocardial border in patients with poor acoustic windows and inappropriate tracking. The lower GLS values on 3DSTE than 2DSTE may be explained by the twisting of the heart and out-of-plane rotation of myocardial segments on 2DE imaging.

As in previous studies (16), we obtained a satisfactory correlation between 2DSTE and 3DSTE for GLS and GCS, but the correlation was poor for GRS. This may be due to the fact that the spatial motion gradient is calculated over a small region in the presence of limited wall thickness and limited spatial image resolution and, additionally, it is estimated not only by endocardial STE data as it occurs for GLS and GCS but by both endocardial and epicardial tracking.

In the present study we defined LV dysfunction as 3D-LV-GLS>-18% on the basis of SDs below the reference limit derived from a group of healthy people. However, different approaches may be used for determining cutoff values of echocardiographic parameters for the different degrees of abnormality, all of which have significant limitations(19). The recognition of clinically significant abnormal values of ventricular strain is not easy because the index is influenced by age, sex, and loading conditions. Current guidelines on chemotherapy-related cardiotoxicity suggest a cardiac assessment based on GLS cutoffs at baseline because a GLS decrease compared to the patient's baseline value is better justified than the use of an absolute cutoff(30,31).

In addition to difference in strain, HAART-treated patients had increased LV mass compared with the control group, as reported in prior studies(5,9,12). They may have had early myocardial damage resulting in subtle scarring and subsequent diastolic dysfunction and impaired deformation parameters. Moreover, they tended to have higher systemic blood pressures, even though not statistically significant, presumably related to the side effects of certain antiretroviral drugs, including endothelial damage, that are associated with early pathologic change in the development of hypertension(32). Increased LV mass in HIV-infected children has been associated with increased mortality(5,12).

Little has been written about LV twist in antiretroviral-treated subjects. In patients with non-ischemic dilated cardiomyopathies and spherically enlarged ventricles it has been reported that LV twist and torsion were significantly impaired inducing LV dyssynchrony(33,34), especially in those with wide QRS complexes(33). Other authors(35) reported no significant difference in twist and torsion between normals and DCM patients, and no correlation with LV ejection fraction. Since the rotational component of the ventricular mechanics involves the endocardium, myocardium, and epicardium, it is presumable that rotational mechanics is preserved in patients with low impact of disease and impaired in more severe cardiomyopathies. In HIV-infected patients LV twist and torsion changes are less well defined. In patients who acquired HIV disease from their mothers antenatally it has been reported significant decrease of LV rotational velocity compared to normal controls(13). We observed in our HIV patients a moderate decrease of apical rotation compared to the control group. Given that early changes in rotational mechanics may occur in the patterns of regional torsion rather than overall magnitude, segmental assessment of twist and torsion could be helpful in identifying deteriorating ventricular function. However, the moderate intra-observer and inter-observer reproducibility of LV twist that we found suggests caution in using this index in clinical practice.

Right ventricle is more complex to quantitate by traditional echocardiography than left ventricle and there has been very little focus on RV toxic HIV effects. HIV-infected patients are at increased risk for pulmonary arterial hypertension and RV cardiomyopathy, warning a poor prognosis(36). The prevalence of PH in HIV-infected patients(36,37) was reported to be 0.5% if documented at right heart catheterization and 5-15% if estimated by echocardiography (PASP>35mmHg). It has been shown that the prevalence of global RV dysfunction in HIV-infected patients was 11% when defined echocardiographically by RV fractional area change <35% and that regional RV dysfunction in HIV may be a distinct entity from high pulmonary pressures or LV cardiomyopathy(37). There are several possible mechanisms of isolated RV dysfunction in HIV,

which include a direct viral toxic effect, genetic variability, opportunistic infections, adverse drug myocardial effects, and autoimmune response.

Three-dimensional STE may improve the difficult assessment of RV dysfunction because of complex spatial ventricular structure. The findings of the present study suggest that 3DSTE identifies mild RV myocardial injury in early stages of the disease as there was no significant relation between the duration of HIV infection and the echocardiographic abnormalities and confirm that RV dysfunction in HIV could be a separate entity as reported in previous 2DSTE studies(37). We found a prevalence of RV dysfunction of 14% (with RVFWLS>-22%). None of our HIV patients had pulmonary hypertension as expressed by PASP>35mmHg albeit we don't have invasive hemodynamic data to confirm the diagnosis of PH. Therefore our findings indicate that HIV cardiomyopathy may only affect one ventricle but may also be biventricular. RV dysfunction was not explained by LV dysfunction and/or LV-RV interaction, because no patient with LV GLS >-18% had RVFWLS >-22% or significant difference in any other measure of RV function. As for LV, even for the right ventricle a clinical advantage of 3DSTE over 2DSTE is a more rapid acquisition and offline-analysis time and a lower intra-observer and inter-observer variability. We have previously shown that the new 3DSTE measurements have strong associations with hemodynamic parameters indicative of RV failure(17). However, none of our HIV-infected patients was symptomatic (NYHA>II), thus values suggesting RV dysfunction in the absence of clinical symptoms are of doubtful significance and should be corroborated by further studies.

Comparison with DCM. All myocardial deformational indices were significantly lower in patients with DCM than in controls, in keeping with previous reports(33-35). Whereas in normal controls the peak systolic strain in different views had a regular pattern, longitudinal and circumferential strain being smallest in the basal region and largest in the apical region, in agreement with previous studies(28,38,39), DCM patients had a disordered strain impairment, with no significant differences between basal and apical regions, and diffuse LV systolic dysfunction. HIV

patients showed an intermediate pattern of impairment of deformation parameters, with moderate strain reduction, predominantly in basal and apical regions.

In normal subjects, the direction of myocardial contractility and shortening reflects the influence of wall stress, i.e. preload, and is consequent to apex-to-base direction of electrical activation. Because the apical myocardial shortening anticipates the shortening of mid-basal regions, the apical region is more heavily affected by the wall stress than the other regions, and longitudinal and circumferential apical shortening is more dynamic in comparison with the basal and mid regions(38). In the dilated cardiomyopathies, as a consequence of the process of ventricular enlargement and remodeling, reduction of cardiac output worsens subendocardial and subepicardial ischemia, and this leads to the replacement of myocardial cells with fibrous tissue and consequent systolic and diastolic cardiac dysfunction. Longitudinal cardiac fibres located in the subendocardium are the first to be affected by myocardial injury, followed by diffuse and disordered strains impairment and intraventricular dyssynchrony. In HIV patients, as in the initial forms of non-ischemic DCM, myocardial segments with preserved systolic function alternate with hypocontractile segments, but these regional abnormalities should not lead to the assumption of coronary artery disease. Segmental LV dysfunction is likely to correspond to the regions where cell myocardial damage is present.

Clinical implications. Our study shows that the integration of the new 3DSTE echocardiographic techniques provide useful information for the assessment of biventricular function in HIV-infected patients in the presence of normal LV ejection fraction and pulmonary artery pressure. Using advanced echocardiographic parameters to assess contractile reserve can help to identify higher-risk individuals, even if the exact significance of strain abnormalities in these patients remains unknown. We don’t know whether this helps to alter clinical decision making or whether drug therapy or device-based treatment that were shown to benefit in heart failure patients without HIV infection would bring benefits to HIV-infected patients as well. Moreover, cumulative toxicities of antiretroviral agents on the heart are poorly studied, and frequent changes in antiretroviral drug

regimens as well as the limited sample size don't allow to correlate the observed cardiac abnormalities to different antiretroviral agents. Additional research is needed to establish long-term prognosis and possibly prevent the development of these abnormalities. However, recommendations on the timing and frequency of cardiac assessment for these patients would be advisable, as well as a collaboration between infectious disease specialists and cardiologists to identify and manage those at high risk of HIV-associated cardiomyopathy.

Limitations. Technical limitations of 3DSTE are the dependence on image quality(40) and its capability to define the endocardial border, the relatively low temporal and spatial resolution, and the fact that the frame rates are not sufficiently high to accurately capture all phases of the cardiac cycle. Further research leading to improvements in both hardware and software is required to assess the feasibility of 3DSTE and the relative importance of current limitations such as the low frame rates.

Secondly, RV strain analysis was done with use of the software aimed for the LV analysis. This methodology has been shown to work in a clinical scenario(17,23), but a dedicated RV 3DSTE software package that takes specific factors into account may be desirable to further improve the feasibility and reproducibility of RV measurements.

Furthermore, although we excluded patients with a history of coronary artery disease, coronary angiography was not performed for all our adult patients. However, stress testing was negative for ischemic heart disease and, additionally, pre-test probability of coronary artery disease is very low in asymptomatic young patients with negative past medical history.

Last, the present study covered only a small number of patients in a single center protocol, thus the results are preliminary and a larger study is required to confirm our findings.

***Conclusions*.** Three-dimensional speckle tracking echocardiography reveals subclinical biventricular dysfunction in young individuals with HIV infection that may be helpful for the early detection of HIV-associated cardiomyopathy in the era of effective ART and long-term survival with chronic HIV. The clinical significance of these findings should be further evaluated.

Conflict of Interest

All authors have no conflict of interest to declare.

References

1. Remick J, Georgiopoulou V, Marti C, et al. Heart failure in patients with human immunodeficiency virus infection: epidemiology, pathophysiology, treatment, and future research. Circulation 2014;129:1781-1789.
2. Savvoulidis P, Butler J, Kalogeropoulos A. Cardiomyopathy and heart failure in patients with HIV infection. Can J Cardiol 2019;35:299-309.
3. Bloomfield GS, Alenezi F, Barasa FA, et al. Human immunodeficiency virus and heart failure in low- and middle-income countries. JACC Heart Fail 2015;3:579-590.
4. Lumsden RH, Bloomfield GS. The causes of HIV-associated cardiomyopathy: A tale of two worlds. Biomed Res Int 2016;2016:8196560.
5. Hsue PY, Hunt PW, Ho JE, et al. Impact of HIV infection on diastolic function and left ventricular mass. Circ Heart Fail 2010;3:132-139.
6. Schuster I, Thöni GJ, Edérhy S, et al. Subclinical cardiac abnormalities in human immunodeficiency virus-infected men receiving antiretroviral therapy. Am J Cardiol 2008;101:1213-1217.
7. Reinsch N, Kahlert P, Esser S, et al. Echocardiographic findings and abnormalities in HIV-infected patients: results from a large, prospective, multicenter HIV-heart study. Am J Cardiovasc Dis 2011;1:176-184.
8. Cunha Mdo C, Siqueira Filho AG, Santos SR, et al. AIDS in childhood: cardiac involvement with and without triple combination antiretroviral therapy. Arq Bras Cardiol 2008;90:11-17.

9. Idris NS, Cheung MM, Grobbee DE, Burgner D, Kurniati N, Uiterwaal CS. Cardiac effects of antiretroviral-naïve versus antiretroviral-exposed HIV infection in children. PLoS One 2016;11(1):e0146753.
10. Gorcsan J 3rd, Tanaka H. Echocardiographic assessment of myocardial strain. J Am Coll Cardiol 2011;58:1401-1413.
11. Vitarelli A, D'Orazio S, Caranci F, et al. Left ventricular torsion abnormalities in patients with obstructive sleep apnea syndrome: an early sign of subclinical dysfunction. Int J Cardiol 2013;165:512-518.
12. Sims A, Frank L, Cross R, et al. Abnormal cardiac strain in children and young adults with HIV acquired in early life. J Am Soc Echocardiogr 2012;25:741-748.
13. Al-Naami G, Kiblawi F, Kest H, Hamdan A, Myridakis D. Cardiac mechanics in patients with human immunodeficiency virus: a study of systolic myocardial deformation in children and young adults. Pediatr Cardiol 2014;35:1046-1051.
14. Mendes L, Silva D, Miranda C, et al. Impact of HIV infection on cardiac deformation. Rev Port Cardiol 2014;33:501-509.
15. Karavidas A, Xylomenos G, Matzaraki V, et al. Myocardial deformation imaging unmasks subtle left ventricular systolic dysfunction in asymptomatic and treatment-naïve HIV patients. Clin Res Cardiol 2015;104:975-981.
16. Vitarelli A, Martino F, Capotosto L, et al. Early myocardial deformation changes in hypercholesterolemic and obese children and adolescents: a 2D and 3D speckle tracking echocardiography study. Medicine 2014;93(12):e71.
17. Vitarelli A, Mangieri E, Terzano C, et al. Three-dimensional echocardiography and 2D-3D speckle tracking imaging in chronic pulmonary hypertension: Diagnostic accuracy in detecting hemodynamic signs of RV failure. J Am Heart Assoc 2015;4(3):e001584.

18. Friis-Møller N, Thiébaut R, Reiss P, et al.; DAD study group. Predicting the risk of cardiovascular disease in HIV-infected patients: the data collection on adverse effects of anti-HIV drugs study. Eur J Cardiovasc Prev Rehabil 2010;17:491-501.
19. Lang RM, Badano LP, Mor-Avi V, et al. Recommendations for cardiac chamber quantification by echocardiography in adults: an update from the American Society of Echocardiography and the European Association of Cardiovascular Imaging. JAmSocEchocardiogr 2015;28:1-39.
20. Lopez L, Colan SD, Frommelt PC, et al. Recommendations for quantification methods during the performance of a pediatric echocardiogram: a report from the Pediatric Measurements Writing Group of the American Society of Echocardiography Pediatric and Congenital Heart Disease Council. J Am Soc Echocardiogr 2010;23:465-495.
21. Rudski LG, Lai WW, Afilalo J, et al. Guidelines for the echocardiographic assessment of the right heart in adults: a report from the American Society of Echocardiography endorsed by the European Association of Echocardiography, a registered branch of the European Society of Cardiology, and the Canadian Society of Echocardiography. J Am Soc Echocardiogr 2010;23:685-713.
22. Nagueh SF, Smiseth OA, Appleton CP, et al. Recommendations for the evaluation of left ventricular diastolic function by echocardiography: An Update from the American Society of Echocardiography and the European Association of Cardiovascular Imaging. J Am Soc Echocardiogr 2016;29:277-314.
23. Mor-Avi V, Lang RM, Badano LP, et al. Current and evolving echocardiographic techniques for the quantitative evaluation of cardiac mechanics: ASE/EAE consensus statement on methodology and indications endorsed by the Japanese Society of Echocardiography. J Am Soc Echocardiogr 2011;24:277-313.

24. Ozawa K, Funabashi N, Takaoka H, et al. Utility of three-dimensional global longitudinal strain of the right ventricle using transthoracic echocardiography for right ventricular systolic function in pulmonary hypertension. Int J Cardiol 2014;174:426-430.
25. Pellikka PA, Nagueh SF, Elhendy AA, Kuehl CA, Sawada SG; American Society of Echocardiography. American Society of Echocardiography recommendations for performance, interpretation, and application of stress echocardiography. J Am Soc Echocardiogr 2007;20:1021-1041.
26. Feinstein MJ, Hsue PY, Benjamin LA, et al. Characteristics, prevention, and management of cardiovascular disease in people living with HIV: A Scientific Statement from the American Heart Association. Circulation 2019;140:e98-e124.
27. Seo Y, Ishizu T, Enomoto Y, et al. Validation of 3-dimensional speckle tracking imaging to quantify regional myocardial deformation. Circ Cardiovasc Imaging 2009;2:451-459.
28. Kaku K, Takeuchi M, Tsang W, et al. Age-related normal range of left ventricular strain and torsion using three-dimensional speckle-tracking echocardiography. J Am Soc Echocardiogr 2014;27:55-64.
29. Stokke TM, Hasselberg NE, Smedsrud MK, et al. Geometry as a confounder when assessing ventricular systolic function: comparison between ejection fraction and strain. J Am Coll Cardiol 2017;70:942-954.
30. Thavendiranathan P, Negishi T, Coté MA, et al.; SUCCOUR Investigators. Single versus standard multiview assessment of global longitudinal strain for the diagnosis of cardiotoxicity during cancer therapy. JACC Cardiovasc Imaging 2018;11:1109-1118.
31. Song FY, Shi J, Guo Y, et al. Assessment of biventricular systolic strain derived from the two-dimensional and three-dimensional speckle tracking echocardiography in lymphoma patients after anthracycline therapy. Int J Cardiovasc Imaging 2017;33:857-868.
32. Xu Y, Chen X, Wang K. Global prevalence of hypertension among people living with HIV: a systematic review and meta-analysis. J Am Soc Hypertens 2017;11:530-540.

33. Matsumoto K, Tanaka H, Tatsumi K, et al. Left ventricular dyssynchrony using three-dimensional speckle-tracking imaging as a determinant of torsional mechanics in patients with idiopathic dilated cardiomyopathy. Am J Cardiol 2012;109:1197-1205.
34. Rady M, Ulbrich S, Heidrich F, et al. Left ventricular torsion - A new echocardiographic prognosticator in patients with non-ischemic dilated cardiomyopathy. Circ J 2019;83:595-603.
35. Balasubramanian S, Punn R, Smith SN, Houle H, Tacy TA. Left ventricular systolic myocardial deformation: A comparison of two- and three-dimensional echocardiography in children. J Am Soc Echocardiogr 2017;30:974-983.
36. Quezada M, Martin-Carbonero L, Soriano V, et al. Prevalence and risk factors associated with pulmonary hypertension in HIV-infected patients on regular follow-up. AIDS 2012;26:1387-1392.
37. Simon MA, Lacomis CD, George MP, et al. Isolated right ventricular dysfunction in patients with human immunodeficiency virus. J Card Fail 2014;20:414-421.
38. Saito K, Okura H, Watanabe N, et al. Comprehensive evaluation of left ventricular strain using speckle tracking echocardiography in normal adults: comparison of three-dimensional and two-dimensional approaches. J Am Soc Echocardiogr 2009;22:1025-1030.
39. Marcus KA, Mavinkurve-Groothuis AM, Barends M, et al. Reference values for myocardial two-dimensional strain echocardiography in a healthy pediatric and young adult cohort. J Am Soc Echocardiogr 2011;24:625-636.
40. Kleijn SA, Aly MF, Terwee CB, van Rossum AC, Kamp O. Reliability of left ventricular volumes and function measurements using three-dimensional speckle tracking echocardiography. Eur Heart J Cardiovasc Imaging 2012;13:159-168.

Figure legends

Figure 1. Representative LV and RV 2D-3D strain images in normal controls and patients with HIV. **A**. 2D LV speckle tracking 4-chamber view in a normal subject. LV global longitudinal strain (LV GLS) is -23.6%. **B**. 3D LV speckle tracking multiplane view in a normal subject. 3D LV GLS is -20.3%. **C**. 3D RV speckle tracking multiplane view in a normal subject. 3D RV global longitudinal strain (RV GLS) is -27.2%. 3D longitudinal strain of RV free-wall (RV FWLS) was then calculated as -28.7% excluding septal segments. **D**. 3D LV speckle tracking multiplane view in a patient with HIV. 3D LV GLS is -16.4%.

Figure 1

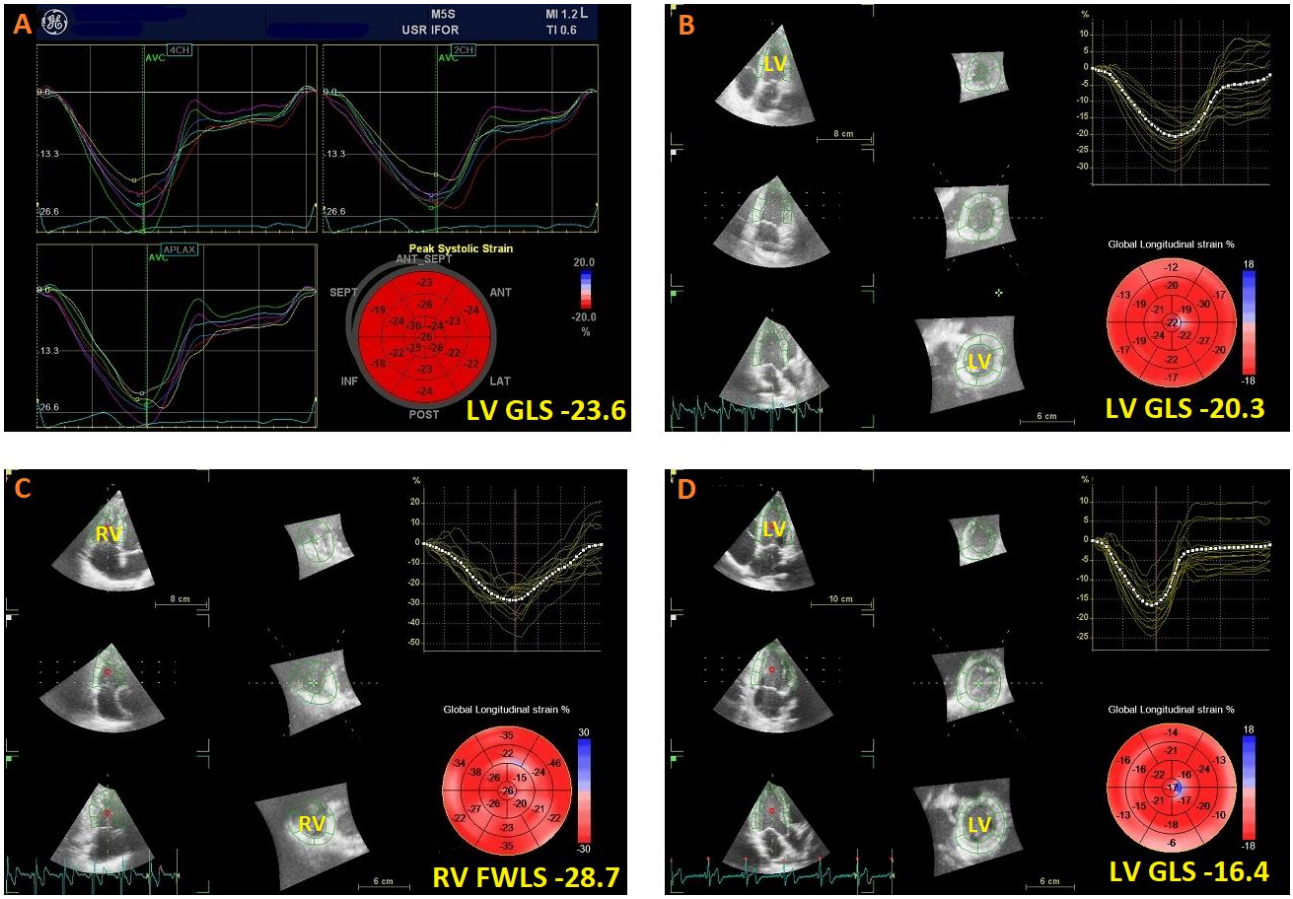
A
M5S
USR IFOR
MI 1.2 L
TI 0.6
4CH
2CH
APLAX
Peak Systolic Strain
ANT_SEPT
SEPT
ANT
INF
LAT
POST
20.0
-20.0
%
LV GLS -23.6
B
LV
LV
8 cm
6 cm
Global Longitudinal strain %
LV GLS -20.3
C
RV
RV
8 cm
6 cm
Global Longitudinal strain %
RV FWLS -28.7
D
LV
LV
10 cm
6 cm
Global Longitudinal strain %
LV GLS -16.4

Table 1. Clinical and laboratory characteristics of the study population

	Controls (n=21)	HIV patients (n=21)	P value
Age (years)	24.1±3.4	23.5±3.8	NS
Gender (M/F)	11/10	11/10	NS
Body surface area (cm^2)	1.76±0.24	1.67±0.19	NS
Body mass index (kg/m^2)	22.6±2.2	22.4±2.6	NS
HR (bpm)	68.6±9.1	66.5±7.8	NS
SBP (mmHg)	120.8±7.1	123.9±6.5	NS
DBP (mmHg)	70.5±5.9	71.8±5.7	NS
Total cholesterol (mg/dL)	155.9±10.9	156.4±11.4	NS
HDL-C (mg/dL)	48.7±8.6	48.1±8.7	NS
LDL-C (mg/dL)	96.9±10.5	97.9±10.3	NS
Triglycerides (mg/dL)	78.8±9.1	79.5±8.4	NS
Age at diagnosis (months)	-	34.5±3.9	-
Duration of disease (years)	-	20.6±2.1	-
Duration of HAART therapy (years)	-	17.5±2.6	-
CD4 nadir (cell/µL)	-	311.8±37.9	-
Actual CD4 count (cell/µL)	-	826.8±79.1	-
DAD risk score	-	2.97±1.35	-

DAD= Data collection on Adverse Effects of Anti-HIV Drugs (ref.18); DBP= diastolic blood pressure; HAART= highly active antiretroviral therapy; HDL= high-density lipoprotein; HR= heart rate; LDL= low-density lipoprotein; NS= not significant; SBP= systolic blood pressure.

Table 2. Conventional echocardiographic findings in HIV-positive patients and controls

Parameters	Controls (n=21) Mean ± SD	HIV patients (n=21) Mean ± SD	P value
LV			
LVED (mm)	48.7±4.2	49.2±4.8	NS
LVES (mm)	29.3±2.5	30.2±3.4	NS
IVST (mm)	9.5±1.8	11.3±1.9	<0.05
LVPWT (mm)	8.7±1.7	10.1±1.8	<0.05
LVMI (g/m^2)	81±19	127±23	<0.05
LVEF (%)	65±5	62±7	NS
DT (msec)	224±49	241±56	NS
MV E_a (cm/s)	11.7±2.3	6.4±3.9	<0.05
MV E/E_a	5.4±1.4	9.3±2.1	0.04
RV			
RVED (mm)	22.6±2.3	24.7±2.6	NS
RVWT (mm)	4.1±0.7	4.2±0.9	NS
RVSP (mmHg)	22±6	24±7	NS
RVEDA (mm^2)	16.3±5.4	20.2±4.1	NS
RVESA (mm^2)	8.2±3.1	9.6±2.3	NS
RVFAC (%)	42±8	40±6	NS
TAPSE (mm)	23±5	19±5	NS
TV S_a (cm/s)	12.4±2.4	11.7±1.8	NS
TV E_a (cm/s)	11.4±2.3	9.7±2.6	0.05
TV E/E_a	4.7±1.1	7.1±1.8	<0.05

DT= deceleration time of early filling; E= inflow early diastolic velocity; E_a= annular early diastolic velocity; LVED= left ventricular end-diastolic diameter (Mmode); LVEDV= left ventricular end-diastolic volume (2D); LVEF= left ventricular ejection fraction (2D); LVES= left ventricular end-systolic diameter (Mmode); LVMI= left ventricular mass index (Mmode); LVPWT= left ventricular posterior wall thickness (Mmode); IVST= interventricular septal thickness (Mmode); MV= mitral valve; NS= not significant; RVED= right ventricular end-diastolic diameter (Mmode); RVEDA= right ventricular end-diastolic area (2D); RVESA= right ventricular end-systolic area (2D); RVFAC= right ventricular fractional area change (2D); RVSP= right ventricular systolic pressure; RVWT= right ventricular wall thickness (Mmode); S_a= annular systolic velocity; TAPSE= tricuspid annular plane systolic excursion; TV= tricuspid valve.

Table 3. Two-dimensional and three-dimensional speckle tracking values in HIV-positive patients and controls

Parameters	Controls (n=21) Mean ± SD	HIV patients (n=21) Mean ± SD	P value
LV 2DSTE			
LV Global LS (%)	-21.4±2.6	-17.2±2.3	<0.05
LV Global CS (%)	-27.7±5.4	-24.9±3.8	<0.05
LV Global RS (%)	48.9±8.3	46.7±7.3	NS
LV peak TW (°)	13.4±4.5	11.6±3.8	<0.05
LV 3DSTE			
3D LVEF	64±7	62±6	NS
LVMI (g/m^2)	72±18	141±27	<0.01
LV Global LS (%)	-20.9±1.5	-14.7±1.9	0.002
LV Basal LS (%)	-19.5±2.1	-14.1±2.3	0.003
LV Mid LS (%)	-20.3±1.9	-15.9±2.5	0.05
LV Apical LS (%)	-23.7±2.5	-18.2±2.7	0.01
LV Global CS (%)	-25.7±3.4	-22.9±3.3	<0.05
LV Global RS (%)	48.6±9.3	35.2±7.9	NS
LV Global AS (%)	-39.8±4.9	-30.3±2.8	0.01
LV peak TW (°)	13.1±4.1	9.2±3.2	0.03
LV peak apical ROT (°)	10.1±3.4	8.2±3.9	0.04
LV peak basal ROT (°)	-5.7±2.5	-4.9±2.4	NS
LV PUV (°/sec)	-99.3±16	-83.7±21	<0.05
LV time to PUV (msec)	395±42	462±44	<0.05
RV 2DSTE			
RV Global LS (%)	-28.4±3.5	-26.5±2.6	NS
RV FW LS (%)	-29.5±3.3	-21.4±3.2	<0.05
RV 3DSTE			
3D RVEF	56±7	54±4	NS
RV Global LS (%)	-26.1±3.9	-19.1±2.8	<0.05
RV FW LS (%)	-28.2±3.1	-18.7±2.9	0.03
RV FW AS (%)	-33.1±5.4	-25.1±5.2	0.04
RV Basal FW LS (%)	-25.8±2.7	-21.5±2.3	NS
RV Mid FW LS (%)	-26.1±4.1	-22.3±3.9	NS
RV Apical FW LS (%)	-26.8±3.9	-19.7±2.2	0.03

AS= area strain; CS= circumferential strain; EF= ejection fraction; FW= free wall; LS= longitudinal strain; LV= left ventricular; LVEF= left ventricular ejection fraction; LVMI= left ventricular mass index; NS= not significant; PUV= peak untwisting diastolic velocity; ROT= rotation; RS= radial strain; RV= right ventricular; RVEF= right ventricular ejection fraction; TW= twist.

Table 4. Differences in segmental 3D left ventricular strain in controls (C), HIV-positive patients (HIV) and patients with idiopathic non-ischemic dilated cardiomyopathy (DCM)

	C (n=21)	HIV (n=21)	DCM (n=21)	p-ANOVA
Longitudinal strain (%)				
Base	-16.39 ± 3.29	-12.41 ± 2.87 ‡ §	-8.61 ± 2.84 #	0.001
Mid	-17.81 ± 3.16 *	-14.27 ± 3.06 §	-6.92 ± 3.09 #	0.005
Apex	-22.85 ± 5.81 †	-11.15 ± 3.27 ‡ §	-8.73 ± 3.18 || #	0.001
Circumferential strain (%)				
Base	-24.85 ± 5.29	-17.95 ± 4.36 ‡ §	-11.35 ± 3.62 #	0.001
Mid	-28.72 ± 5.62 *	-25.88 ± 4.94 §	-10.08 ± 4.39 #	0.005
Apex	-32.47 ± 10.73 †	-18.19 ± 4.71 ‡ §	-9.87 ± 5.47 || #	0.001
Radial strain (%)				
Base	33.34 ± 7.65	25.41 ± 6.59 §	11.63 ± 4.86 #	0.005
Mid	38.57 ± 8.59 *	26.28 ± 7.03	9.82 ± 4.75 #	0.001
Apex	31.54 ± 9.71	24.63 ± 6.59 ||	8.62 ± 4.49 || #	0.005
Area strain (%)				
Base	-42.45 ± 7.82	-30.52 ± 7.76 ‡ §	-12.51 ± 4.74 #	0.001
Mid	-43.23 ± 6.94 *	-34.64 ± 6.83 §	-16.46 ± 5.28 #	0.005
Apex	-45.61 ± 7.18 †	-31.76 ± 6.35 §	-16.93 ± 5.45 || #	0.001

NS= not significant

C: * $p<0.05$ vs basal region, † $p<0.05$ vs mid region *(normal base-apical strain gradient*)

HIV: ‡ $p<0.05$ vs mid region, § $p<0.05$ vs controls (*moderate localized strain impairment*)

DCM: || p= NS vs basal and mid region, # $p<0.001$ vs controls (*severe diffuse strain impairment*)

Table 5. Reproducibility of 2DSTE and 3DSTE parameters

	Intraobserver results				Interobserver results			
Variable	Mean difference ± SD	ICC	CV (%)	P value	Mean difference ± SD	ICC	CV (%)	P value
2D-LVGLS, %	7.5±3.4	0.89	2.61	0.002	8.7±3.7	0.87	2.11	0.01
2D-LVGCS, %	8.8±3.2	0.83	1.27	0.03	9.8±3.5	0.81	1.23	0.04
2D-LVGRS, %	11.7±4.4	0.79	1.53	0.05	12.9±4.3	0.78	1.16	0.05
2D-LVTW, °	13.1±4.1	0.82	1.65	0.05	14.2±4.4	0.77	1.73	0.05
2D-RVGLS, %	7.3±3.3	0.81	1.94	0.02	8.4±4.3	0.80	2.37	<0.05
2D-RVFWLS, %	6.9±3.1	0.86	2.03	0.004	7.5±3.6	0.85	1.82	0.03
3D-LVGLS, %	6.7±2.2	0.95	2.92	<0.001	7.4±2.6	0.91	2.43	0.002
3D-LVGCS, %	7.7±2.8	0.87	1.44	0.02	8.5±2.7	0.83	1.85	0.03
3D-LVGRS, %	9.8±4.2	0.81	2.13	0.04	10.3±3.7	0.79	3.57	0.05
3D-LVGAS, %	5.8±2.4	0.95	3.16	<0.001	6.2±2.7	0.92	2.88	0.001
3D-LVTW, °	12.4±3.8	0.86	2.41	0.03	13.2±3.9	0.79	3.57	0.04
3D-RVGLS, %	7.1±2.5	0.82	2.54	0.01	7.8±3.5	0.81	2.77	0.02
3D-RVFWLS, %	6.8±2.3	0.89	2.12	0.003	7.2±3.3	0.85	1.89	0.03

3D= three-dimensional; 2D= two-dimensional; CV= coefficient of variation (calculated as the difference of repeated measurements expressed as a percentage of the mean); ICC= intraclass correlation coefficient for absolute agreement; LVGAS= left ventricular global area strain; LVGCS= LV global circumferential strain; LVGLS= LV global longitudinal strain; LVGRS= LV global radial strain; LVTW= left ventricular twist; ns= not significative; RVFWLS= right ventricular free-wall longitudinal strain; RVGLS= right ventricular global longitudinal strain.